Journal of Medicinal Chemistry
Brief Article

J. Med. Chem. **2010,** *53,* 1867–1870 **1867**
DOI: 10.1021/jm9017515

Structure of Human G Protein-Coupled Receptor Kinase 2 in Complex with the Kinase Inhibitor Balanol†

John J. G. Tesmer,*,‡,§ Valerie M. Tesmer,‡ David T. Lodowski,∥,∞ Henning Steinhagen,⊥ and Jochen Huber⊥

‡*Life Sciences Institute, and* §*Department of Pharmacology, University of Michigan, Ann Arbor, Michigan 48109-2216,* ∥*Department of Chemistry and Biochemistry, Institute for Cellular and Molecular Biology, The University of Texas at Austin, Austin, Texas 78712, and* ⊥*Sanofi-Aventis Deutschland GmbH, D-65926 Frankfurt am Main, Germany.* ∞*Current address: Department of Pharmacology, Case Western Reserve University, Cleveland, Ohio 44106.*

Received November 25, 2009

G protein-coupled receptor kinase 2 (GRK2) is a pharmaceutical target for the treatment of cardiovascular diseases such as congestive heart failure, myocardial infarction, and hypertension. To better understand how nanomolar inhibition and selectivity for GRK2 might be achieved, we have determined crystal structures of human GRK2 in complex with G$\beta\gamma$ in the presence and absence of the AGC kinase inhibitor balanol. The selectivity of balanol among human GRKs is assessed.

Introduction

G protein-coupled receptor (GPCR[a]) kinases (GRKs) phosphorylate activated GPCRs and thereby initiate their uncoupling from heterotrimeric G proteins and their internalization.[1,2] The seven mammalian GRKs (GRK1−7) are grouped into three subfamilies: GRK1 (GRK1 and -7), GRK2 (GRK2 and -3), and GRK4 (GRK4−6).

Although GRK2 is expressed in many tissues, it seems particularly important for embryonic development and heart function, and elevated GRK2 activity is associated with both heart failure and hypertension.[3] Thus, it is believed that therapeutic inhibition of GRK2 would improve cardiovascular function. Structural analysis of bovine GRK2 (bGRK2) has led to several crystal structures, including complexes with Gα_q and G$\beta\gamma$ heterotrimeric G proteins.[4−6] However, a well-ordered ligand in the active site has not yet been reported, perhaps because in all of these structures the kinase domain adopts an "open", presumably inactive conformation in which the nucleotide-binding site is not fully formed.

The natural product balanol (Figure 1a) is a potent, albeit relatively nonselective inhibitor of AGC kinases.[7] X-ray crystal structures of balanol and balanol analogues bound to PKA reveal that the compound binds to a conformation of PKA that is intermediate to the "open" (inactive) and "closed" (active) states of the kinase.[8−10] Herein we report that GRKs are also potently inhibited by balanol and that the drug exhibits some selectivity among GRK subfamilies. We describe the structure of the human GRK2 (hGRK2)−G$\beta\gamma$·balanol complex. Comparison with the ligand-free structure reveals that balanol stabilizes the kinase domain of GRK2 in a slightly more closed conformation distinct from that of the PKA·balanol complex.

Results

Inhibition Assays. We assessed the ability of balanol to inhibit kinase activity for all seven GRK family members using biotinylated tubulin dimers as a substrate. As shown in Table 1, the IC_{50} of balanol was ∼50 nM for GRK2 and GRK3 but higher for members of the GRK1 and GRK4 subfamilies. GRK6 was inhibited with the least potency ($IC_{50} \approx 500$ nM). The IC_{50} for PKA under similar conditions was 110 nM (data not shown).

Structure of the hGRK2−G$\beta\gamma$ Complex. hGRK2 and bGRK2 differ by only 11 conservative substitutions, allowing the hGRK2−G$\beta\gamma$ complex to crystallize under the same conditions as bGRK2−G$\beta\gamma$. The native crystal structure was solved using diffraction data to 2.75 Å spacings (Table S1 of Supporting Information). hGRK2 and bGRK2 superimpose well, with a root mean squared deviation (rmsd) of 1.1 Å for 612 equivalent Cα positions. The most prominent difference between the two structures is the conformation of the flexible α5−α6 loop region of the regulator of G protein signaling homology domain.

Conformational Changes upon Binding Balanol. The hGRK2−G$\beta\gamma$·balanol complex was formed by soaking pre-existing crystals or by cocrystallization with balanol (Figure 1b). The resulting crystal structures superimpose with an rmsd of 0.2 Å for 617 Cα positions, indicating that both procedures yield an essentially identical ligand-bound state. The binding of balanol induces conformational changes in the hGRK2 kinase domain (0.6 Å rmsd for 310 Cα atoms between the apo and balanol complexes), including a 4° closure of the large lobe relative to the small lobe

†Protein coordinates and structure factors for the hGRK2−G$\beta\gamma$, hGRK2−G$\beta\gamma$·balanol (soak), and hGRK2−G$\beta\gamma$·balanol (cocrystal) complexes have been deposited with the Protein Data Bank with PDB codes 3CIK, 3KRW, and 3KRX, respectively.

*To whom correspondence should be addressed. Address: Life Sciences Institute, 210 Washtenaw Avenue, University of Michigan, Ann Arbor, Michigan, 48109-2216. Phone: (734) 615-9544. Fax: (734) 763-6492. E-mail: johntesmer@umich.edu.

[a]Abbreviations: AGC, protein kinase A, kinase G, and kinase C subfamily; bGRK2, bovine G protein-coupled receptor kinase 2; DTT, dithiothreitol; G, GTP-binding protein; GPCR, G protein-coupled receptor; GRK, G protein-coupled receptor kinase; hGRK2, human G protein-coupled receptor kinase 2; PKA, protein kinase A; rmsd, root mean squared deviation.

Published on Web 02/03/2010

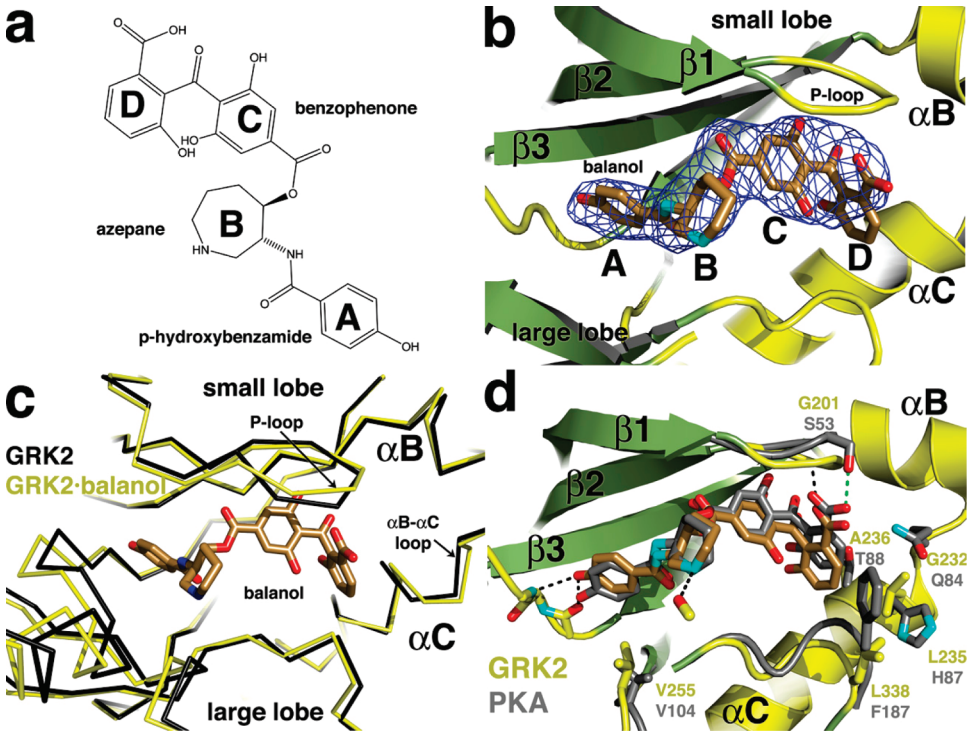

Figure 1. Balanol and the hGRK2·balanol complex. (a) Chemical structure of balanol, with A, B, C, and D rings labeled. (b) Balanol bound in the active site of hGRK2. Electron density from a 2.9 Å $|F_o| - |F_c|$ omit map (blue cage) is drawn at the 3σ level. Balanol is drawn with carbons colored tan, oxygens red, and nitrogens cyan. (c) Comparison of apo hGRK2 (black Cα trace) with hGRK2·balanol (yellow Cα trace). The small lobes of the structures were superimposed. Conformational changes are observed in the P-loop and in the αB−αC loop of the small lobe, and the kinase domain adopts a slightly more closed conformation when in complex with balanol. (d) Comparison of the hGRK2·balanol and PKA·balanol complexes. The PKA·balanol complex (PDB entry 1BX6) is shown with gray carbons. hGRK2-Val255 is displaced into the binding pocket relative to its equivalent in PKA (Val104), forcing an upward tilt of the A ring. The benzophenone moiety is displaced toward the large lobe (bottom of figure) relative to PKA. Residues that contact the benzophenone moiety in hGRK2 are substituted by shorter side chains relative to PKA: hGRK2-Gly201 (PKA-Ser53) in the P-loop, hGRK2-Gly232 (PKA-Gln84) in αB, hGRK2-Leu235 (PKA-His87) and hGRK2-Ala236 (PKA-Thr88) in αC, and hGRK2-Leu338 (PKA-Phe187) in the large lobe. Hydrogen bonds between hGRK2 and balanol are shown with black dashed lines. One hydrogen bond, shown in green, is unique to the PKA complex.

Table 1. Inhibition (IC_{50}, nM) of Tubulin Phosphorylation by Balanol[a]

GRK1	GRK2	GRK3	GRK4	GRK5	GRK6	GRK7
340	42	47	260	160	490	180

[a] IC_{50} values were measured in duplicate. The average is shown.

around an axis running roughly parallel to the longest dimension of the kinase domain (Figure 1c). On the basis of the transition-state-like structure of PKA,[11] we estimate that an additional 16° rotation is required to achieve a fully closed state. Subtle conformational changes are also observed within the small lobe (0.5 Å rmsd for 108 Cα atoms). Cα atoms in the $\beta1-\beta2$ (P-loop) and αB−αC loops move up to 1.6 and 1 Å, respectively, away from the active site relative to the apo hGRK2 structure, apparently to help accommodate balanol (Figure 1c). The large lobe of hGRK2 does not undergo significant conformational changes upon binding the inhibitor (0.3 Å rmsd for 201 Cα atoms).

Comparison with the PKA·Balanol Complex. Conformational and sequence-specific differences between PKA and hGRK2 cause these kinases to bind balanol in distinct ways. Differences in the degree of kinase domain closure cause the pocket accommodating the A ring to be more compressed in GRK2 relative to PKA, whereas the pocket occupied by the benzophenone (C and D) rings appears larger (Figure 1d). In hGRK2, the A ring is tilted away from the large lobe relative to its position in the PKA·balanol complex such that its hydroxyl is displaced by 1.4 Å. This is due, in part, to the side chain of hGRK2-Val255, which projects further into the nucleotide binding pocket than the equivalent valine in PKA (Figure 1d). The position of hGRK2-Val255 is in turn influenced by the more open conformation of the GRK2 kinase domain and a three-residue insertion in the αC−$\beta4$ loop (hGRK2 residues 246−255) relative to PKA.

In the hGRK2 structure, balanol binds such that the D ring is positioned up to 1.4 Å closer to the large lobe of the kinase compared to its position in the PKA·balanol complex (Figure 1d). Consequently, the P-loop of hGRK2, which forms hydrogen bonds and apolar contacts with the benzophenone moiety, is drawn 1.4 Å closer to the large lobe than is the P-loop of PKA. Residues in PKA that contact the benzophenone ring are larger than their equivalents in GRK2, causing the balanol binding site of PKA to appear more compact (Figure 1d). However, these sequence differences do not appear to greatly diminish the inhibitory potency of balanol.

Balanol itself exhibits significant conformational differences when bound to PKA and hGRK2, demonstrating its ability to adapt to unique active site environments. Rotations are observed in the bonds linking the azepane group (B ring) to the adjacent rings and in the bond linking the D ring to the rest of the benzophenone moiety.

Discussion

GRKs are atypical members of the AGC kinase family in that their kinase domains require the docking of activated GPCRs to stabilize their catalytically active state. Indeed, crystal structures of GRK2,[4] GRK6,[12] and GRK1[13] reveal that in the absence of GPCRs the kinase domains of these proteins exist in relatively open, presumably inactive conformations compared to the nucleotide bound forms of other AGC kinases.[14,15] Although nucleotides induce a small degree of domain closure in the case of GRK1, the effect is still insufficient to fully coalesce its active site machinery.[13] Therefore, one reason balanol exhibits some selectivity among GRKs, but not among the broader AGC kinase subfamily, may be that balanol is required to adapt to the distinct inactive conformations exhibited by these GRK subfamilies, whereas other AGC kinases can more readily adopt conformations similar to that of the PKA·balanol complex.

We docked balanol into structures of GRK1 and GRK6 to identify some potential sources of selectivity (Figure S1 in Supporting Information). The binding site for the A ring is more open and perhaps less optimal in GRK1 and GRK6 relative to GRK2. Nonconserved positions in the active site that contact balanol may also influence selectivity. For example, hGRK2-Leu235 in the αC helix directly interacts with the D ring but is substituted by Gly231 in GRK1 and Met231 in GRK6 (Figures 1d and S1). Ile197 in the β1 strand directly contacts the A ring but is substituted by leucine in the GRK1 and GRK4 subfamilies.

In PKA, the binding of balanol causes the kinase domain to close by 9°, as opposed to the 4° closure we observe in hGRK2. The resulting balanol-bound conformations of these enzymes are thus distinct. Despite this, balanol is flexible enough to bind with relatively high affinity to either active site. Our results suggest that inhibitors with less flexibility than balanol could be designed to enhance selectivity for GRKs because the inactive states of these enzymes have distinct conformations from each other and from PKA.[13] Indeed, drugs that target unique inactive states of other protein kinases have proven remarkably effective.[16]

Experimental Section

Materials. Balanol was produced by cultivating the fungus strain ST003555 (from Gabon, Africa) on solid rice plates and 10% malt medium at 25 °C for 14 days. After methanol extraction, the proteins were fractionated on MCI Gel (Mistsubishi Chemical Company; CHP20P, 75−150 μm) and the pooled fractions containing balanol were further purified (>95%) with reverse phase HPLC.[17] Biotinylated bovine tubulin dimers were obtained from TEBU-BIO Offenbach, Germany. GRK2−7 proteins for IC_{50} determination were obtained from Invitrogen, and bovine heart PKA (catalytic subunit) was from Sigma. GRK1 was produced by Sanofi-Aventis GmbH.

Inhibition of GRK2-Mediated Tubulin Phosphorylation. GRKs 1−7 with specific activity of 450 (pmol/min)/mg were first incubated with various concentrations of balanol (100, 20, 4, 0.8, 0.16, 0.032, 0.064, and 0.00128 μM) for 30 min at room temperature in assay buffer (20 mM Tris-HCl, pH 7.4, 2 mM EDTA, and 2.25% DMSO). The phosphorylation reactions were started by adding $MgCl_2$ (10 mM), ATP (3 μM), [γ-^{33}P]-ATP (0.4 μCi/40 μL), and the GRK·balanol complex to biotinylated bovine tubulin dimers (250 nM) coated on 384-well StreptaWell plates (Roche). The reaction was stopped after 30 min by adding 0.8% BSA, 0.8% Triton X100, 80 mM EDTA, and 400 μM ATP at 4 °C and then incubated for 18 h. After a final wash with PBS, pH 8.0, the amount of bound ^{33}P-labeled tubulin was quantified by scintillation counting (60 μL Ultima Gold MV scintillation fluid per well) using a Microbeta TriLux microplate scintillation counter (Perkin-Elmer).

Purification and Crystallization of hGRK2−G$\beta\gamma$. Geranylgeranylated bovine G$\beta_1\gamma_2$ was expressed in High Five insect cells and purified as previously described.[18] hGRK2 was expressed in a 6 L of fermenter using the baculovirus expression system in Sf9 cells and was purified as described previously for bGRK2.[18] Crystallization experiments used the second of two peaks that eluted from the Source S cation exchange column, which corresponds to the unphosphorylated form of hGRK2 and 80−85% of the total hGRK2.[19]

To produce native crystals, the hGRK2−G$\beta\gamma$ complex was purified by gel filtration chromatography in the presence of 1 mM ATP as described for bGRK2−G$\beta\gamma$.[18] For crystallization, 1 μL of 7.8 mg/mL hGRK2−G$\beta\gamma$ complex and 1 μL of well solution (100 mM MES, pH 5.25 or 6.0, 200 mM NaCl, 5% ethylene glycol, and 6.3% PEG 3350) were mixed in a drop suspended over 1 mL of well solution at 4 °C. Crystals appeared within 10 days and reached maximum dimensions (0.3 mm × 0.15 mm × 0.05 mm) in 20 days. Crystals were serially transferred from a harvesting solution containing 100 mM MES, pH 6.0, 200 mM NaCl, 10 mM CHAPS, 1 mM ATP, 2 mM $MgCl_2$, 20 mM HEPES, pH 8.0, and 1 mM DTT into the same solution, omitting ATP and containing in addition 15% ethylene glycol and 10% DMSO in steps of 3.25% and 2.5%, respectively.

For cocrystallization with balanol, the hGRK2−G$\beta\gamma$ complex was purified by gel filtration in the absence of ATP and concentrated to 8.4 mg/mL before adding balanol (50 mM stock in 100% DMSO) to a final concentration of 500 μM. The protein was crystallized under conditions similar to those of the native complex, with the largest crystals obtained in a well solution of 100 mM MES, pH 6.0, 200 mM NaCl, 9% PEG 3350. Crystals were harvested in 20 mM HEPES, pH 8, 300 mM NaCl, 10 mM CHAPS, 5 mM $MgCl_2$, 12%PEG3350, 2 mM DTT, 100 mM MES, pH 6.0, 250 μM balanol, 0.5% DMSO, and 25% ethylene glycol.

For soaks with balanol, native crystals were harvested by slow addition of a solution containing 100 mM MES, pH 5.6, 300 mM NaCl, 12% PEG 3350, 10 mM CHAPS, 5 mM $MgCl_2$, 20 mM HEPES, pH 8.0, 2 mM DTT, and 25% ethylene glycol to the hanging drop. The crystals were then serially transferred into harvesting solution that included 250 μM and then 2.5 mM balanol, giving a final concentration of 5% DMSO. Crystals were then incubated overnight at 4 °C.

Data Collection and Structure Determination. Diffraction data from crystals harvested on cryoloops (Hampton Research) and maintained at 110 K were collected on CCD detectors at beam lines 19-BM and 21-ID-G at the Advanced Photon Source (APS). Data were integrated and scaled using *HKL2000*. Initial phases were provided by molecular replacement using the bGRK2-G$\beta\gamma$ complex structure (PDB code 1OMW) as a search model. The final model was built using successive rounds of manual model building with the program O and maximum-likelihood refinement in *REFMAC5*. Data collection and refinement statistics are provided in Table S1.

Acknowledgment. We thank M. Dreyer for the crystal soaking protocol, M. Lohse for the hGRK2 baculovirus, I. Focken for Sf9 expression of hGRK2, and C. Presenti and L. Toti for balanol fermentation and purification. Use of LS-CAT sector 21 was supported by the Michigan Economic Development Corporation and the Michigan Technology Tri-Corridor (Grant 085P1000817). Use of the Advanced Photon Source was supported by the U.S. Department of Energy, Office of Science, Office of Basic Energy Sciences, under Contract DE-AC02-06CH11357.

Supporting Information Available: Additional methods, Table S1, and Figure S1. This material is available free of charge via the Internet at http://pubs.acs.org.

References

(1) Pitcher, J. A.; Freedman, N. J.; Lefkowitz, R. J. G protein-coupled receptor kinases. *Annu. Rev. Biochem.* **1998**, *67*, 653–692.

(2) Claing, A.; Laporte, S. A.; Caron, M. G.; Lefkowitz, R. J. Endocytosis of G protein-coupled receptors: roles of G protein-coupled receptor kinases and β-arrestin proteins. *Prog. Neurobiol.* **2002**, *66*, 61–79.

(3) Dorn, G. W., 2nd. GRK mythology: G protein receptor kinases in cardiovascular disease. *J. Mol. Med.* **2009**, *87*, 455–463.

(4) Lodowski, D. T.; Pitcher, J. A.; Capel, W. D.; Lefkowitz, R. J.; Tesmer, J. J. Keeping G proteins at bay: a complex between G protein-coupled receptor kinase 2 and G$\beta\gamma$. *Science* **2003**, *300*, 1256–1262.

(5) Tesmer, V. M.; Kawano, T.; Shankaranarayanan, A.; Kozasa, T.; Tesmer, J. J. Snapshot of activated G proteins at the membrane: the Gα_q−GRK2−G$\beta\gamma$ complex. *Science* **2005**, *310*, 1686–1690.

(6) Lodowski, D. T.; Barnhill, J. F.; Pyskadlo, R. M.; Ghirlando, R.; Sterne-Marr, R.; Tesmer, J. J. The role of G$\beta\gamma$ and domain interfaces in the activation of G protein-coupled receptor kinase 2. *Biochemistry* **2005**, *44*, 6958–6970.

(7) Setyawan, J.; Koide, K.; Diller, T. C.; Bunnage, M. E.; Taylor, S. S.; Nicolaou, K. C.; Brunton, L. L. Inhibition of protein kinases by balanol: specificity within the serine/threonine protein kinase subfamily. *Mol. Pharmacol.* **1999**, *56*, 370–376.

(8) Narayana, N.; Diller, T. C.; Koide, K.; Bunnage, M. E.; Nicolaou, K. C.; Brunton, L. L.; Xuong, N. H.; Ten Eyck, L. F.; Taylor, S. S. Crystal structure of the potent natural product inhibitor balanol in complex with the catalytic subunit of cAMP-dependent protein kinase. *Biochemistry* **1999**, *38*, 2367–2376.

(9) Breitenlechner, C. B.; Wegge, T.; Berillon, L.; Graul, K.; Marzenell, K.; Friebe, W. G.; Thomas, U.; Schumacher, R.; Huber, R.; Engh, R. A.; Masjost, B. Structure-based optimization of novel azepane derivatives as PKB inhibitors. *J. Med. Chem.* **2004**, *47*, 1375–1390.

(10) Akamine, P.; Madhusudan; Brunton, L. L.; Ou, H. D.; Canaves, J. M.; Xuong, N. H.; Taylor, S. S. Balanol analogues probe specificity determinants and the conformational malleability of the cyclic 3′,5′-adenosine monophosphate-dependent protein kinase catalytic subunit. *Biochemistry* **2004**, *43*, 85–96.

(11) Madhusudan; Akamine, P.; Xuong, N.-H.; Taylor, S. S. Crystal structure of a transition state mimic of the catalytic subunit of cAMP-dependent protein kinase. *Nat. Struct. Biol.* **2002**, *9*, 273–277.

(12) Lodowski, D. T.; Tesmer, V. M.; Benovic, J. L.; Tesmer, J. J. The structure of G protein-coupled receptor kinase (GRK)-6 defines a second lineage of GRKs. *J. Biol. Chem.* **2006**, *281*, 16785–16793.

(13) Singh, P.; Wang, B.; Maeda, T.; Palczewski, K.; Tesmer, J. J. Structures of rhodopsin kinase in different ligand states reveal key elements involved in G protein-coupled receptor kinase activation. *J. Biol. Chem.* **2008**, *283*, 14053–14062.

(14) Knighton, D. R.; Zheng, J. H.; Ten Eyck, L. F.; Ashford, V. A.; Xuong, N. H.; Taylor, S. S.; Sowadski, J. M. Crystal structure of the catalytic subunit of cyclic adenosine monophosphate-dependent protein kinase. *Science* **1991**, *253*, 407–414.

(15) Yang, J.; Cron, P.; Good, V. M.; Thompson, V.; Hemmings, B. A.; Barford, D. Crystal structure of an activated Akt/protein kinase B ternary complex with GSK3-peptide and AMP-PNP. *Nat. Struct. Biol.* **2002**, *9*, 940–944.

(16) Noble, M. E.; Endicott, J. A.; Johnson, L. N. Protein kinase inhibitors: insights into drug design from structure. *Science* **2004**, *303*, 1800–1805.

(17) Kulanthaivel, P.; Hallock, Y. F.; Boros, C.; Hamilton, S. M.; Janzen, W. P.; Ballas, L. M.; Loomis, C. R.; Jiang, J. B. Balanol: a novel and potent inhibitor of protein kinase C from the fungus *Verticillium balanoides*. *J. Am. Chem. Soc.* **1993**, *115*, 6452–6453.

(18) Lodowski, D. T.; Barnhill, J. F.; Pitcher, J. A.; Capel, W. D.; Lefkowitz, R. J.; Tesmer, J. J. Purification, crystallization and preliminary X-ray diffraction studies of a complex between G protein-coupled receptor kinase 2 and G$\beta_1\gamma_2$. *Acta Crystallogr., Sect. D: Biol. Crystallogr.* **2003**, *59*, 936–939.

(19) Pitcher, J. A.; Tesmer, J. J.; Freeman, J. L.; Capel, W. D.; Stone, W. C.; Lefkowitz, R. J. Feedback inhibition of G protein-coupled receptor kinase 2 (GRK2) activity by extracellular signal-regulated kinases. *J. Biol. Chem.* **1999**, *274*, 34531–34534.